Evolution Study of the Surface States of Low Carbon Microalloyed Steel before and after Corrosion in NaCl Solution

Faouzia Benkafada[1,*], *Djahida* Kerdoud[2], and *Ali* Bouchoucha[1]

[1]University of Constantine 1, Department of Mechanical Engineering, Constantine, Algeria
[2]University Centre Abdelhafid Boussouf, Mila, Algeria

Abstract. Surface topography is of paramount interest in science, technology, and industry. In this work investigation of the evolution of the surface with multiparameter characterization was carried out using optical profiler. Surface profile is measured two-dimensionally applying Gaussian filter of cutoff 0.8 mm. R_a, R_q, R_{sk}, R_{ku}, R_p, R_v and R_z values according to the standard ISO 4287 were measured. Following ISO 25178, 3D roughness parameters: S_a, S_q, S_{sk}, S_{ku}, S_p and S_v values were reported. The appearance of the texture of our microalloyed steel has been indicated by evaluating the texture aspect S_{tr}. Analysis of Abott-Firestone curves and related parameters S_{mr} and S_{dc} was presented. Some significant characterization parameters such as surface hardness, weight loss and corrosion rate were analysed and compared.

1 Introduction

Currently, the micro-alloyed steels have emerged as an important class of materials and drawn lots of research focus. They are called micro-alloyed steels because they contain only a small number of alloying elements such as: vanadium, niobium or titanium [1-2]. In addition, they have a ferritic matrix with extremely fine grained structure due to the effects of the alloying elements [3]. Consequently, micro-alloyed steels are generally characterized by high strength and ductility resulting from the fine grains and ferrite matrix. They are thus widely used in the oil and gas industry due to their beneficial mechanical properties.
In recent years, there is a growing awareness of the necessity to evaluate the surface quality. The surface roughness is recognized as being one of the most important properties. A wide range of roughness parameters can be used to describe a given surface [4-5]. The most common parameters are calculated from line profiles according to the ISO 4287 standard [6], but due to an increased use of 3D profilers a set of complimentary area roughness parameters have been defined in the ISO 25178 standard [7].

In the present study, an effort has been made to determine the surface properties of micro-alloyed steels by analysing the change in several 3D parameters. In addition, microstructural evaluation, surface hardness measurements, weight loss, and corrosion rate were performed and considered in order to assess the suitability of such steels for application to gas transmission pipelines.

2 Experimental details

2.1 Materials

The steel used in this study is a low carbon ferritic steel with a ferrite-pearlite fine-grained microstructure. In delivery condition, the steel manifests approx. 86.64 ferrite and 13.35 pearlite, with a measured average grain size of ASTM 8 (see Table 1) [8].

Table 1. Composition of as-received steel.

Steel	Ferrite	Pearlite	ASTM grain
Vol%	86.64	13.35	8

The chemical composition is detailed in Table 2 [8].

Table 2. Chemical composition (in wt.%) of the steel used in the experiment.

Steel	C	Mn	Si	P	S	Cr	Cu	Ni	F
Wt.%	0.111	0.955	0.175	0.005	0.022	0.037	0.293	0.013	98.3

2.2 Metallographic preparation

In order to perform the gravimetric measurements, pipeline tests of Ø12 diameter were machined into a rectangular form of 25 mm × 15 mm × 4.45 mm. Specimens were subjected to a mechanical polishing at a speed of 500 rpm using the silicon carbide abrasive papers sequentially of up to 1000 grades, the polished surface was then thoroughly rinsed with distilled water and degreased in acetone before used and dried with an electric drying machine. All experiments were carried out under thermostatic conditions 25°C (±0.1°C).

* Corresponding author: fbenkafadar@yahoo.fr

2.3 X-ray diffraction

The XRD analysis was performed using X'Pert3 Powder Diffractometer. Diffraction patterns were recorded at 45 kV and 40 mA in 0.013°/s detector's movement speed, the scanning was carried out with a step length of 3.35° (2θ) and a step time of 29.07 s. Flat diffracted beam pyrolitic graphite monochromator was used to remove fluorescent X-rays. It becomes very relevant when analyzing iron compounds with CuKα radiation. Noise that emerges because of the fluorescence (without monochromator) would be so large that only the most intensive diffraction maximums (e.g. from ferrite) would appear in the diffraction pattern. The diffraction patterns were recorded automatically by a data acquisition system. The peaks obtained were identified with those available in PDF-2 data base.

2.4 Surface roughness measurements

An optical profilometer, AltiSurf® 500, was used to characterize the roughness of the sample. Using the software, Phenix V2, cartographies of the disc surfaces were done with 5x5 mm dimensions. An acquisition with steps of 2 micron, a speed of 400 micron/sec and a double frequency 400/800 Hz. Roughness profiles of a 4.9 mm length were extracted from the diagonal of the cartographies and their parameters (R_a, R_z, etc.) were calculated with Altimap topography XT software. Optical images were captured by a CCD camera and then recorded.

2.5 Weight loss measurements

The samples were tinted with anti-rust paint all over the sides except around one facade that is to be buried in the ground at pH from 7 to 9. After weighing with sensitive electronic balance, samples were immersed in 10 ml 0.9% NaCl solutions. Weight loss of metal samples was noted at every 24 h time interval. The experiments were carried out in duplicate and the average values were reported.
After the completion of the test, the corrosion rate is calculated by the following equation:

$$V = \Delta M / S.\ T\ (mg/h.\ cm^2) \qquad (1)$$

Where:

V : corrosion rate (mg/h.cm²)
S : the total area of specimen (cm²)
T : time of immersion (h)
$\Delta M = M_i - M_f$ (mg)
ΔM : the average weight loss (mg)
M_i : initial mass (mg)
M_f : final mass (mg)

2.6. Hardness testing

Vickers hardness of metallographic samples were evaluated using a digital Vickers microhardness and Wolpert UH930 Universal Hardness testing machines. Tests were carried out in three different positions on the polished surface of the samples and the average Vickers hardness value was reported.

3 Results and discussion

3.1 X-ray diffraction analysis

X-ray diffraction patterns (Fig. 1) of the samples, that were used in microscopic analysis, are quite similar, and all visible very sharp diffraction peaks, that have interplanar spacings $d(110)$ = 0.2027 nm; $d(200)$ = 0.14336 nm and $d(211)$ = 0.1171 nm, belong to ferrite (α-Fe) cubic lattice. There are no other diffraction peaks, also typical to carbide phase. This confirmed the literature data that carbide phase in the steel could be identifiable by XRD only if there are 5 or more percents of it.

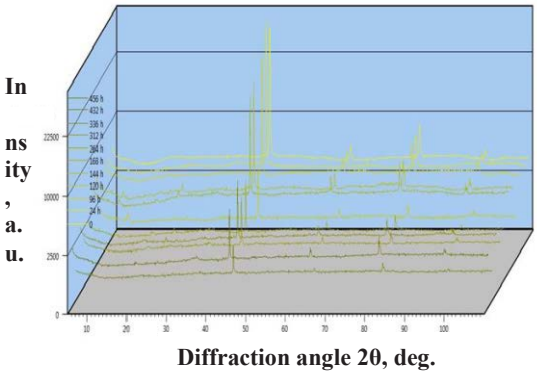

Fig. 1. X-ray diffraction patterns of the steel. Curves : 1 - 0 h, 2 - 24 h, 3 - 96 h, 4 - 120 h, 5 - 144 h, 6 - 168 h, 7- 264 h, 8 - 312 h, 9 - 336 h, 10 - 432 h, 11 - 456 h.

It can be seen that there were not any significant changes in the amount of each phase formed, and as the time exposure is extended, the intensity of the peaks corresponding to ferrite increases slightly, this indicates that the interplanar space was smaller.

3.2 Optical profiler analysis

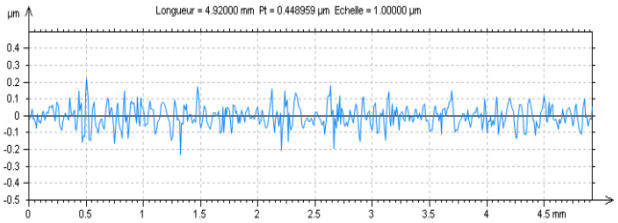

Fig. 2. 2D roughness profile of sample obtained after 144 h of immersion into NaCl solution.

Using a simple 2D profile, as shown in Fig. 2, may not provide a complete picture of the sample surface. This profile can provide accurate height, width and roughness data, but may miss detailed surface features that can be measured by adding 3D analysis capabilities.
According to ISO 4287**,** 2D amplitude parameters values are shown in Table 3.

For sample immersed for 144 h, it is important to note that the sum of R_P and R_V is equal to R_Z, which is lower than the value R_t. This result is in good agreement with the literature given by the ISO 4287 standard.

Table 3. 2D amplitude parameters.

ISO 4287		
2D amplitude parameters		
R_p	0.152645	µm
R_v	0.140306	µm
R_z	0.292951	µm
R_c	0.143695	µm
R_t	0.403858	µm
R_a	0.0446722	µm
R_q	0.0563578	µm
R_{sk}	-0.021757	
R_{ku}	3.47164	
Functional parameters – Roughness profile		
R_{mr}	100.000	%
R_{dc}	0.0907388	µm

With 3D capabilities, an entire area can be mapped, as shown in Fig. 3. This enables visual inspection of defects and uniformity.

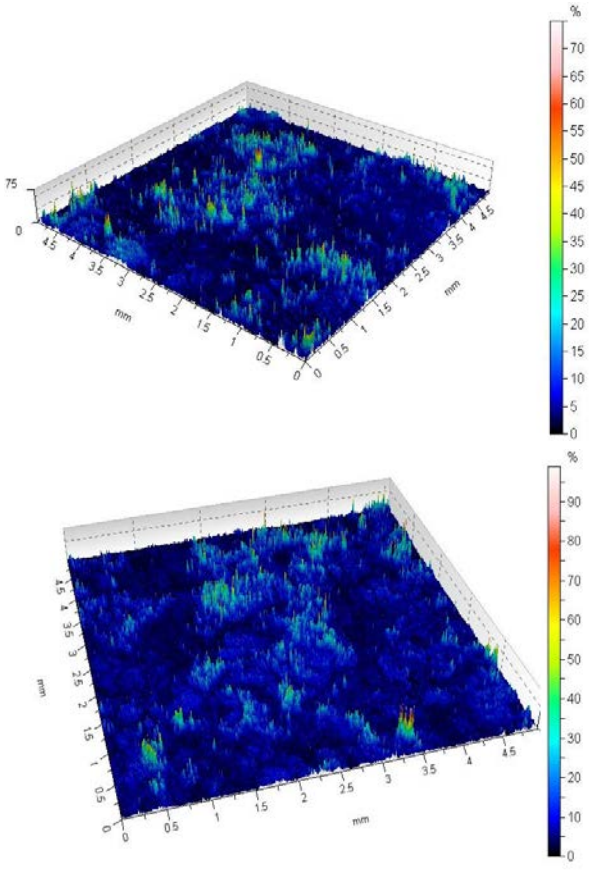

Fig. 3. 3D surface roughness image of samples obtained after 144 h and 168 h of immersion into NaCl solution, respectively.

3D roughness images for the patterned samples showed shiner blue colour after corrosion, where small surface pits and spikes could appear depending on the two basic parameters, immersion time into NaCl solution and localized area of corrosion. Other colours show deep point like grooves.

Following ISO 25178, 3D surface roughness parameters are indicated in Table 4.

Table 4. 3D height parameters.

ISO 25178		
Height parameters		
S_q	0.835091	µm
S_{sk}	0.315758	
S_{ku}	10.8696	
S_p	10.4655	µm
S_v	9.70796	µm
S_z	20.1734	µm
S_a	0.539842	µm

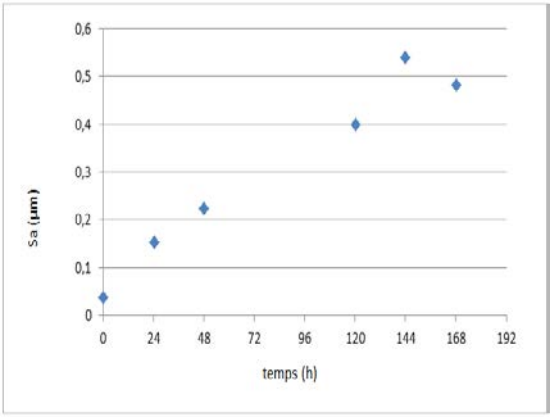

Fig. 4. Variation of arithmetic mean height S_a with immersion time into NaCl.

It is observed from Fig. 4 that an increase in arithmetic mean height S_a is accompanied by an enhancement of the corrosion. Interestingly, this trend is similar to that in the variation of corrosion rate with corrosion period (Fig. 8). It can be concluded that the corrosion rate increased with an increase of surface roughness. The reason of this phenomenon is that by increasing the roughness the active sites increased and deeper grooves played an active role as suitable places for localized corrosion. The depth of the valleys that influenced the diffusion of active ions during NaCl corrosion.
By contrast, in a smooth surfaces weak points are less activate than on rough surface and the formation of stable passive film on smooth surfaces is more likely to occur.

A bearing ratio analysis was performed on both types of samples as seen in Fig. 5. A bearing ratio curve indicates the percentage of a surface that falls above/below a particular depth. These curves quantified the percentage of valley area that tended to lead to corrosion.

Skewness and valley depth were found to correlate well with the tendency toward corrosion. Furthermore, a ratio of parameters derived from the bearing area analysis proved an excelent indicator of the tendency to corrode.

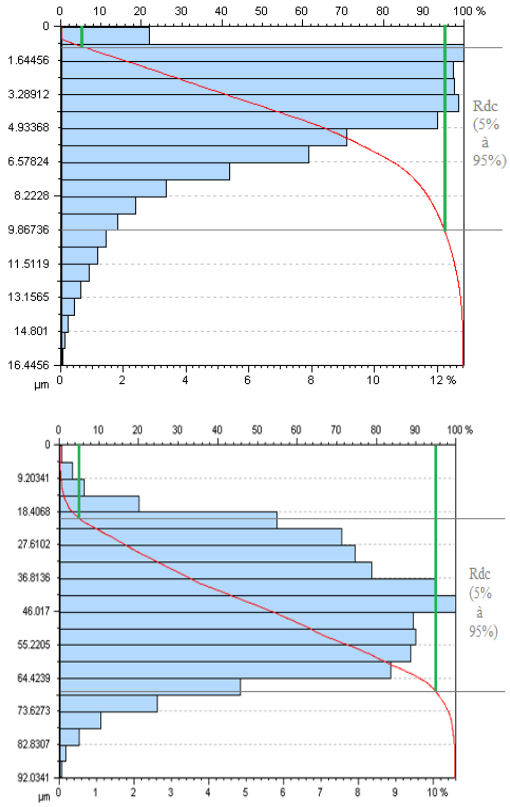

Fig. 5. Abott-Firestone curves before and after 144 h of immersion into NaCl, respectively.

Table 5. The bearing ratio values.

	Before corrosion	After 144 h of immersion into NaCl
5 % to 95% (µm)	9.04508	48.31795

From these data prsented in Table 5, it was determined that the deeper valley structure tended to hold processing NaCl solutions, allowing rusting to occur.

Surface anisotropy is also observed with the 3D roughness parameter S_{tr} ratio of texture aspect. The value can lie in the interval from 0 to 1. It can be concluded that the appearance of the surface texture after 144 h of immersion into NaCl solution is of the anisotropic type while the steel as-received is essentially isotropic before corrosion.

3.3 Hardness evaluation

Table 6. Vickers micro-hardness results.

As-received (HV)	151.0	161.6	156.4
After immersion into NaCl (HV)	66.8	78.3	81.46

After calculation, the average micro-hardness with a load of 4.903 N is found:
• Initial condition (as-received) : 156.33 HV
• After immersion into NaCl : 75.52 HV
Micro-hardness values have changed slightly from 151 to 156.4 and there is a decrease in the hardness of the surface layer after immersion into NaCl solution. It can be attributed to ferrite phase, it is expected that some ferrite zone have been formed in the microstructure of the steel. This can be related to the role of Si element (0.175%). Presence of Si element as ferrite stabilizer in the composition of the steel.

3.4 Weight loss and corrosion rate measurements

The results obtained for the variation of weight loss and corrosion rate with exposure time, with varied concentrations of NaCl solution are presented in Table 7.

Table 7. Weight loss and corrosion rate variations with immersion period and NaCl concentration.

Time (h)	Mass (g)	Weight loss (mg)	NaCl Concentration (mg/ml)	Corrosion rate (mg/h.cm^2)
0	11.67104	0	0	0
24	11.66680	4.24	10	0.04711
48	11.66027	10.77	20	0.05983
144	11.63080	40.24	40	0.07452
168	11.62938	41.66	50	0.06612

It must be pointed out that in the initial condition (steel as-received) no weight loss was seen. However, there is a significant variance between the weight losses of the samples tested in different chloride concentrations that has noteworthy effect on the weight loss of micro-alloyed steel.

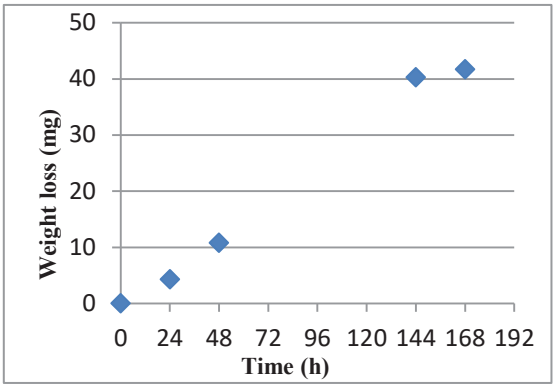

Fig. 6. Variation of weight loss with time exposure.

It is seen from the table that the samples lose weight with increasing exposure time. The observed increase in cumulative weight loss of the samples at constant temperature agrees with the observation made that corrosion rate increases with increasing immersion period time in NaCl solution, while the observed variation in the weight loss of the sample may be

attributed to difference in the samples grain size [9]. It was equally revealed that concentration of NaCl affects rate of corrosion and posited that the bigger the grains of material, the more are its resistance to corrosion [10]. Hence, the as-received sample with the biggest grain size distribution revealed less weight loss as compared to the samples immersed in NaCl solution.
The NaCl medium with 10 mg/ml concentration had the least corrosion effect of the immersed samples by the end of the 24th hour achieving a weight loss value of 4.24 mg. At this value it could be considered to be fairly protective. The NaCl medium with 50 mg/ml concentration recorded the highest weight loss with a value of 41.66 mg showed that the NaCl exhibited very good corrosion at the end of the 168th hour. Additionally, it was further observed that the exposure time had greater significant effect on the corrosion rate.

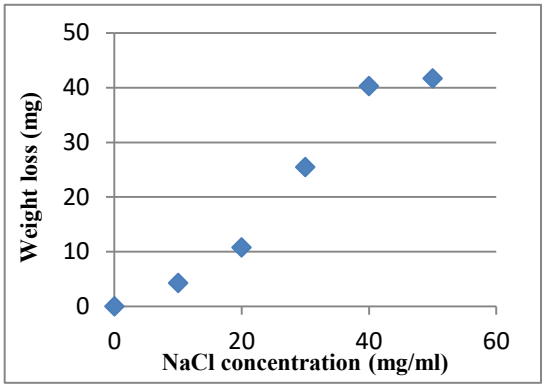

Fig. 7. Effect of NaCl concentration on weight loss.

Ferritic steels having a softer matrix can be easily and rapidly corroded by corrosion reactions depending on the time. On the other hand, hardness of the steel matrix provides good chemical and mechanical properties. Chloride ions induce localized corrosion on carbon steels and can as well lead to the formation of significant amount of corrosion products on steels [11].

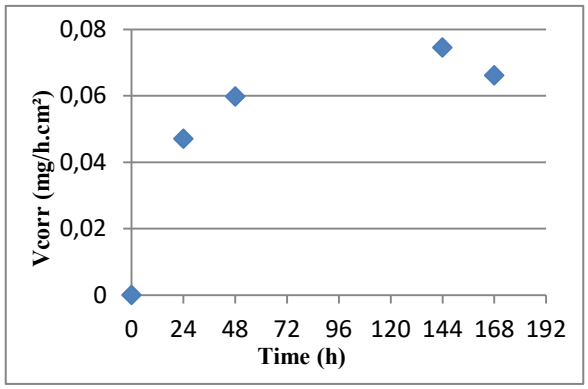

Fig. 8. Variation of corrosion rate with immersion time into NaCl.

Our results show that the corrosion rate of the steel increases sharply and then decreases to stabilize at a value close to 0.07012 (mg/h.cm²) due to the presence of a passive film. Most corrosion-resistant metals and alloys are in the passive state [12], which confirms our results.
Due to the presence of the passive film, the passive dissolution which corresponds to a certain potential is slower than the active dissolution. It depends, inter alia, on the properties of the film, in particular its solubility in the electrolyte. During passivation, in other words during the transition from the active to the passive state, the dissolution rate decreases [13], which is in good agreement with our results.
The increasing degradation of micro-alloyed steel due to chloride as detected in this study compares well with outcomes on corrosion performance of carbon steel. However, micro-alloyed steel may be supposed to be basically well-suited for gas transmission pipelines application since its corrosion rates are characteristically low.

4 Conclusions

Based on the experimental results, the following conclusions can be drawn from the present investigation:
i. The XRD technique enables to identify the phases formed and the intensity of those peaks defines the amount of the steel phases. The microstructure of the samples consists of fine ferrite. The amount of ferrite reduced with hardness due to corrosion in NaCl solution.
ii. Weight loss of the samples is determined as a function of immersion period into NaCl solution. The results show that the microstructure and micro-hardness at different exposure time directly affect the corrosion rate, as the micro-hardness decreases the corrosion rate increases. The samples displayed higher corrosion rate. The presence of a passive film provides a higher protection characteristic.
iii. Sodium chloride concentration of up to 50 mg/ml increases the weight loss. Chloride further increases the corrosion rate. In the absence of chloride, no weight loss and corrosion rate were observed.
iv. Many parameters have been established regarding the measurement and assessment of surface roughness. Surface parameters have been shown to exert a great influence on corrosion and corrosion rate where the amplitude parameters have the most significant effect.
v. Micro-alloyed steel is supposed to be well-suited for gas transmission pipelines application due to its very low corrosion rate.

References

[1] M. Korchynsky, Proc. Conf. on Microalloying Union Carbide Corp., New York, (1977) 75.
[2] Yakubtsov I.A., Poruks P. and Boyd J.D. (2008) Microstructure and mechanical properties of bainitic low carbon high strength plate steels. Mater Sci Eng A, 480, 109-116.
[3] Seikh EM, Seikh AH. Effects of grain refinement on the corrosion behavior of micro-alloyed steel in sulfuric acid solutions. Int J Electrochem Sci (2012); 7:7567-78.

[4] F. Szigeti, Gy. Varga, G. Dezső, L. Péter, A. Százvai: Forgácsolási paraméterek felületi érdességre gyakorolt hatása környezetkímélő megmunkálásoknál, MTÉAR (Műszaki Tudomány az Észak-Alföldi Régióban) 2010 konferencia, Nyíregyháza, 2010 Május 19. kiadvány, p.193-198. (ISBN 978-963-7064-24-1, ISBN 978-963-7064-23-4).
[5] F. Szigeti, Gy. Varga, G. Dezső: Experimental investigation on roughness of drilled surfaces resulted from environmentally conscious machining, International Journal of Engineering, VIII. (2010) 3. pp.: 313-317. ISSN: 1584-2073.
[6] ISO 4287 – Geometrical product specifications (GPS) - Surface texture : Profile method - Terms, definitions and surface texture parameters (1997).
[7] Geometrical product specifications (GPS) - Surface texture: Areal - Part 2: Terms, definitions and surface texture parameters (ISO 25178-2:2012).
[8] Seminar IAP 24; "Corrosion et Protection des Canalisations", 28-03-2013.
[9] D. T. Oloruntoba, O. O. Oluwole, and E. O. Oguntade, "Comparative study of corrosion behaviour of galvanized steel and coated Al 3103 roofing sheets in carbonate and chloride environments," Materials and Design, vol. 30, no. 4, pp. 1371-1376, (2009).
[10] G. H. Aydogdu and M. K. Aydinol, "Determination of susceptibility to intergranular corrosion and electrochemical reactivation behaviour of AISI 316L type stainless steel," Corrosion Science, vol. 48, no. 11, pp. 3565-3583, (2006).
[11] Roman J, Vera R, Bagnara M, Carvajal AM, Aperador W. Effect of chloride ions on the corrosion of galvanized steel embedded in concrete prepared with cements of different composition. Int J Electrochem Sci (2014); 9:580-92.
[12] H. Bentrah, Master dissertation, University of Biskra, 2007.
[13] K. Mohamed Lakhdar, Master dissertation, "détérioration des canalisations sous l'effet des différents facteurs de la corrosion", University of Biskra, 2014.